



# HHS Public Access

Author manuscript

*Nat Cell Biol.* Author manuscript; available in PMC 2012 October 01.

Published in final edited form as:

*Nat Cell Biol.* ; 14(4): 386–393. doi:10.1038/ncb2454.

## Whacked and Rab35 polarize dynein motor complex-dependent seamless tube growth

Jodi Schottenfeld-Roames and Amin S. Ghabrial\*

Department of Cell & Developmental Biology, University of Pennsylvania School of Medicine, 421 Curie Blvd., 1214 BRB II/III, Philadelphia, PA 19104

### Abstract

Seamless tubes form intracellularly without cell-cell or autocellular junctions. Such tubes have been described across phyla, but remain mysterious despite their simple architecture. In *Drosophila*, seamless tubes are found within tracheal terminal cells, which have dozens of branched protrusions extending hundreds of microns. We find that mutations in multiple components of the dynein motor complex block seamless tube growth, raising the possibility that the luminal membrane forms through minus-end directed transport of apical membrane components along microtubules. Growth of seamless tube is polarized along the proximodistal axis by Rab35 and its apical membrane-localized GAP, Whacked. Strikingly, loss of *whacked* (or constitutive activation of Rab35) leads to tube overgrowth at terminal cell branch tips, while overexpression of *whacked* (or dominant negative Rab35) causes formation of ectopic tubes surrounding the terminal cell nucleus. Thus, vesicle trafficking plays key roles in making and shaping seamless tubes.

---

Three tube types – multicellular, autocellular and seamless – are found in the *Drosophila* trachea<sup>1, 2</sup>. Most tracheal cells contribute to multicellular tubes or make themselves into unicellular tubes by wrapping around a luminal space and forming autocellular adherens junctions, but two specialized tracheal cell types, fusion cells and terminal cells, make “seamless” tubes.<sup>1, 3, 4</sup> How seamless tubes are made and how they are shaped is largely unknown. One hypothesis holds that seamless tubes are built by “cell hollowing,”<sup>5, 6</sup> in which vesicles traffic to the center of the cell and fuse to form an internal tube of apical membrane, while an alternative model proposes that apical membrane is extended internally from the site of intercellular adhesion.<sup>7</sup> In both models, transport of apical membrane would likely play a key role. Because terminal cells make seamless tubes continuously during larval life, they serve as an especially sensitive model system in which to dissect the genetic program.

---

Users may view, print, copy, download and text and data- mine the content in such documents, for the purposes of academic research, subject always to the full Conditions of use: [http://www.nature.com/authors/editorial\\_policies/license.html#terms](http://www.nature.com/authors/editorial_policies/license.html#terms)

\*Author for correspondence: ghabrial@mail.med.upenn.edu, (215) 898-7805 (phone), (215) 898-9871 (FAX).

### AUTHOR CONTRIBUTIONS

JS-R and ASG conceived of and carried out all experiments described here. ASG wrote the manuscript with input from JS-R. Figures were assembled by JS-R and ASG.

Tracheal cells are initially organized into epithelial sacs with their apical surface facing the sac lumen. During tubulogenesis,  $\gamma$ -tubulin becomes localized to the luminal membrane of each tracheal cell, generating microtubule networks oriented with minus-ends towards the apical membrane.<sup>8</sup> Terminal and fusion cells are first selected as tip cells<sup>1</sup> that undergo a partial epithelial to mesenchymal transition and initiate branching morphogenesis: they lose all but one or two cell-cell contacts and become migratory.<sup>9, 10</sup> Branchless-FGF signaling induces a subpopulation of tip cells to differentiate as terminal cells.<sup>9</sup> During larval life, terminal cells ramify on tissues spread across several hundred microns, with branching patterns that reflect local hypoxia.<sup>11</sup> A single seamless tube forms within each branched extension of the terminal cell.

How trafficking contributes to seamless tube morphogenesis is unknown. Despite clues that vesicle transport plays a role in the genesis of seamless tubes, the tube morphogenesis genes remain elusive.<sup>7, 11–13</sup> Here we characterize the cytoskeletal polarity of larval terminal cells, show that a minus-end directed microtubule motor complex is required for seamless tube growth, and characterize mutations in *whacked* that uncouple seamless tube growth from the normal spatial cues. Sequence analysis suggests that *whacked* encodes a RabGAP, and we show that Rab35 is the essential target of Whacked, and that together, Whacked and Rab35 can polarize the growth of seamless tubes.

We examined apical-basal polarity and cytoskeletal organization in mature larval terminal cells. The luminal membrane (Figure S1a, b and Methods) was decorated by puncta of Crumbs, a definitive apical membrane marker<sup>14, 15</sup> (Figure 1a, a', b, b'). We found actin filaments enriched in three distinct subcellular domains: surrounding seamless tubes, decorating filopodia, and outlining short stretches of basolateral membrane (Figure 1c-c'', d-d''). The microtubule cytoskeleton also appeared polarized, with  $\gamma$ -tubulin lining the seamless tubes and enriched at tube tips (Figure 2a-a'', b-b''). These data are consistent with tracheal studies in the embryo.<sup>7</sup> EB1::GFP analyses of growing (plus-ends) microtubules demonstrated that some are oriented towards the soma and others towards branch tips (Movie S1). Stable acetylated microtubules ran parallel to the tubes (Figure 2d-d'') and extended beyond the lumen at branch tips (Figure 2c-c'', arrowhead) where they may template tube growth. Consistent with such a role, we observed microtubule tract-associated fragments of apical membrane distal to the blind ends of the seamless tubes (Figure 2c-c'', arrow). Filopodia extended past the stable microtubules (Figure 2e-e'', white arrowhead) as expected. These data suggest that mature terminal cells maintain the polarity and organization described for embryonic terminal cells.<sup>7</sup> Based on  $\gamma$ -tubulin localization, we infer that a subset of microtubules is nucleated at the apical membrane, and that apically-targeted transport along such microtubules would require minus-end motor proteins. Indeed, homozygous mutant *Lissencephaly-1* (*Lis-1*, a Dynein motor-associated protein) embryos have been reported to have seamless tube defects.<sup>7</sup> Because  $\gamma$ -tubulin lines the entire apical membrane, growth through minus-end directed transport might be expected to occur all along the length of seamless tubes, and indeed, a pulse of CD8::GFP (transmembrane protein tagged with GFP) synthesis uniformly labeled the apical membrane as it first became detectable (Figure S1c, c' and supplemental methods).

The cytoplasmic Dynein motor complex drives minus-end directed transport of intracellular vesicles in many cell types;<sup>16</sup> to test for its requirement in seamless tube formation, we examined terminal cells mutant for any of four dynein motor complex genes: Dynein heavy chain 64C (*Dhc64C*), Dynein light intermediate chain (*dlic*), Dynactin p150 (*Glued*), and *Lis-1*. Mutant terminal cells showed a cell autonomous requirement for these genes. Mutant terminal cells had thin cytoplasmic branches that lacked air-filling (Figure 3a–e'), and antibody staining revealed that seamless tubes did not extend into these branches although acetylated microtubules often did (Figure 3f–i and data not shown). We also note that formation of filopodia at branch tips is disrupted in dynein motor complex mutants, which may account for the decreased number of branches in mutant terminal cells. Ectopic seamless tubes that were not air-filled were detected near the nucleus, as described below. Interestingly, discontinuous apical membrane fragments (similar to those in *Lis-1* embryos)<sup>7</sup> were found in terminal branches lacking seamless tubes, and were associated with microtubule tracts (Figure 3h,i). While  $\gamma$ -tubulin was enriched on truncated tubes and on these presumptive seamless tube intermediates, diffuse  $\gamma$ -tubulin staining was detected throughout the mutant cells (Figure 3j, j'; compare to Figure 2a, b), suggesting that assembly of apical membrane is required to establish or maintain  $\gamma$ -tubulin localization. Likewise, Crumbs appeared reduced and aberrantly localized (Figure S1d–f). Reduced acetylated microtubule staining in these cells may reflect loss of apical  $\gamma$ -tubulin (compare 3h, i). Importantly, these data show that stable microtubules extend through cellular projections that lack seamless tubes. Thus, without minus-end directed transport, stable microtubules are insufficient to promote seamless tube formation, but stable cellular projections are formed and maintained in the absence of seamless tubes.

In contrast to these defects in seamless tubes generation, mutations in *whacked*<sup>17</sup> confer overly exuberant tube growth (Figure 3k,l and Figure S2a, d, i). Examination of *whacked* terminal cell tips revealed a “U-turn” phenotype in which seamless tubes executed a series of 180 degree turns – below we entertain the possibility that branch retraction, similar to that observed in talin mutants,<sup>18</sup> could contribute to the U-turn defect.

Homozygous *whacked* animals survived until pharate adult stages, and other than the seamless tube defects, had normal tracheal tubes at the third larval instar. Mosaic analysis revealed a terminal cell autonomous requirement for *whacked*. Mutant clones in multicellular tubes, and in unicellular tubes that lumenize by making autocellular adherens junctions, were of normal morphology (Figure S2f–h). Strikingly, fusion cells, which also form seamless tubes, were unaffected by loss of *whacked*.

To determine the molecular nature of *whacked* we took a positional cloning approach (Figure S3 and methods). Mapping techniques defined a candidate gene interval of ~ 75 kb. We focused on CG5344 as it encodes a protein containing a TBC (Tre2/Bub2/Cdc16) domain characteristic of Rab GTPase activating proteins (GAPs),<sup>19–21</sup> and hence was likely to participate in vesicular trafficking, a process that could lie at the heart of seamless tube formation. We identified single nucleotide changes that result in mis-sense (PC24) and nonsense (220) mutations in CG5344 coding sequence. Pan-tracheal knockdown of *whacked* by RNAi caused terminal cell-specific U-turn defects (other defects characteristic of the EMS alleles of *whacked* -- see supplemental methods – were detected at a low frequency,

data not shown). A genomic rescue construct for CG5344 rescued *whacked* mutants, confirming gene identity (Figure S2j, m). Based on these results, we conclude that *whacked* is CG5344 and that it likely regulates vesicular trafficking during seamless tube morphogenesis.

To determine the Rab target(s) of Whacked regulation, we tested whether tracheal expression of constitutively active “GTP-locked” Rab isoforms (henceforth Rab-CA) might phenocopy *whacked*. Rab-CA for 31 of the 33 *Drosophila* Rabs<sup>22</sup> were tested individually in the tracheal system. Rab35-CA alone conferred terminal cell-specific U-turns defects (Figure 4a–g).

To evaluate Whacked over-expression, UAS-*whacked* (methods) was expressed in wild type animals in a pan-tracheal pattern. Excess Whacked caused formation of ectopic seamless tubes surrounding the terminal cell nucleus (proximal seamless tube overgrowth) (Figure 4h). At higher levels of expression, small spheres of apical membrane were found adjacent to the nucleus and less abundantly at more distal sites (Figure S4a–l). Consistent with Whacked regulation of vesicle trafficking by modulation of Rab35, expression of a dominant negative Rab35 (henceforth, Rab35-DN) caused formation of ectopic proximal tubules (Figure 4i, j).

We sought to determine whether Rab35 was the essential target of Whacked GAP activity. Whacked primary structure is equally conserved in three human RabGAPs: TBC1D10C (FLJ00332 /Carabin/EPI64C – 32% identity), TBC1D10A (EPI64A – 30% identity), and TBC1D10B (FLJ13130/ EPI64B – 27% identity). All three act as Rab35GAPs,<sup>23</sup> although each has been proposed to have additional targets<sup>24–26</sup>. To further test if Whacked acts as a Rab35GAP, we examined whether Rab35DN could suppress *whacked* mutants; tracheal-specific expression of Rab35DN strongly suppressed the “U-turn” defects of *whacked* null animals and surprisingly, also rescued the lethality of *whacked* (Figure S2k, m). Since mutant Rab35 isoforms phenocopy *whacked* gain and loss of function, Rab35DN bypasses the requirement for *whacked*, and human Whacked orthologs are Rab35GAPs, we conclude that the critical function of Whacked is as a GAP for *Drosophila* Rab35.

In other systems Rab35 is implicated in polarized membrane addition to plasma membrane compartments – e.g immune synapse, cytokinetic furrow, etc. – or, in actin regulation.<sup>23, 27–36</sup> Because a role for actin in fusion cell seamless tube formation has been proposed,<sup>37</sup> we examined whether Whacked and Rab35 act by modulation of the terminal cell actin cytoskeleton. Because the actin bundling protein Fascin (*Drosophila singed*) was recently identified biochemically as a Rab35 effector,<sup>36</sup> we tested for a role of *singed* in terminal cell tubes, but found no evidence for one (methods, Figure S4m–r).

Furthermore, over-expression of Whacked (Figure S4t), or of Rab35DN (data not shown), did not significantly alter the terminal cell actin cytoskeleton, leading us to conclude that actin regulation is not a primary function of Wkd/Rab35 during seamless tube morphogenesis.

We found the alternative model – that Rab35 acted in polarized membrane addition – attractive, since extra Rab35-GTP activity promoted seamless tube growth at branch tips

whereas depletion of Rab35-GTP promoted tube growth at the cell soma. To test this model, we took advantage of our knowledge that expression of an activated Breathless-FGFR ( $\lambda$ -Btl)<sup>38</sup> in terminal cells induces robust growth of ectopic seamless tubes surrounding the nucleus (Figure 4k and Figure S5a, e); we asked if growth of the ectopic tubes could be redirected from the soma to the branch tips by eliminating *whacked*. The activated FGFR phenotype was not altered in *whacked* heterozygotes (Figure S5b, e), but in *whacked* mutant animals (or *whacked* RNAi animals) the site of ectopic seamless tube growth was strikingly different. In some cells, extra tubes were found throughout the cell (Figure S5d, e) – in the soma and at branch tips – while in others extra tubes were only present at the branch tip (Figure 4l, Figure S5c, e). Thus, the position of seamless tube growth is dependent upon Whacked activity, although Whacked itself is not essential for tube formation. These data argue against branch retraction (as occurs in talin mutants)<sup>18</sup> as the mechanism for generating a U-turn phenotype, since branch retraction would not re-direct ectopic tube growth.

To better understand how Whacked and Rab35 determined the site of seamless tube growth, we investigated their subcellular distribution. Pan-tracheal expression of mKate2 tagged Whacked (Wkd::mKate) rescued *whacked* null animals (Figure S2l, m). The steady-state subcellular localization of Wkd::mKate was restricted to the luminal membrane with higher accumulation at the growing tips of seamless tubes (direct fluorescence of Wkd::mKate in a fixed larva, Figure 5a). At lower levels, we noted cytoplasmic puncta of Wkd::mKate that could reflect vesicular localization, and labeling of filopodia (immunofluorescence using an antibody against mKate; Figure 5b,c). We found that YFP-Rab35 was distributed in a diffuse pattern throughout the terminal cell cytoplasm with some apical enrichment, and notable localization to filopodia (Figure 5b', d). We find substantial co-localization of Wkd::mKate with YFP::Rab35 at the apical membrane, in cytoplasmic puncta, and in filopodia (Figure 5b''). Among endosomal Rabs, Rab35 appeared uniquely abundant within filopodia, and showed the greatest overlap with Whacked at the apical membrane (Figure S4u-x). We noted substantial overlap between Wkd/Rab35 and acetylated microtubules, including at positions distal to the blind-end of seamless tubes (Figure 5b'', c, d, e). The enrichment of Whacked along seamless tubes suggests that Rab35 functions in an apical membrane trafficking event, leading us to speculate that recycling endosomes at filopodia might be targeted to the growing seamless tube by minus-end motor transport.

In a similar vein, we speculate that vesicles might be transported from the soma towards branch tips in a process regulated by Whacked and Rab35. Disruption of such transport might explain why over-expression of *whacked* leads to ectopic seamless tube growth in the soma. We asked if Wkd::mKate localization was compromised in dynein motor complex mutants. Because these cells have branches that lack apical membrane/seamless tubes, we anticipated disruption in the localization pattern of Wkd, but wondered whether co-localization with acetylated tubulin would be intact, indicative of a microtubule association independent of dynein motor transport. We find that Wkd::mKate2 is broadly distributed throughout the cytoplasm of dynein motor complex mutants, and does not show enrichment on acetylated microtubule tracts (Figure 5f,f', g, g'), indeed, we detected substantial basal enrichment of Wkd::mKate. If Whacked/Rab35 dependent trafficking of apical vesicles was

dynein motor complex dependent, we might expect to see ectopic seamless tubes in the soma of dynein motor complex mutants, similar to those seen with *whacked* over-expression or expression of DN-Rab35. In fact, we consistently find such ectopic tubes in the dynein motor complex mutants (Figure 5h–k), consistent with dynein-dependent trafficking of Rab35 vesicles. We cannot rule out the possibility that these defects are due to dynein-dependent processes unrelated to Wkd and Rab35; however, we did test whether the ectopic tubes could be redirected distally by expression of CA-Rab35, or elimination Wkd (Figures S1g–g'', h–h''). The motor complex ectopic tube phenotype could not be altered, suggesting that the phenotype does not arise as an indirect consequence of altered Wkd localization or Rab35 activity.

The roles of RabGAP proteins have only started to come into focus in recent years. Historically, it has been difficult to determine which Rab proteins are substrates of specific RabGAPs.<sup>39</sup> Tests of *in vitro* GAP activity produced conflicting results, and in some cases did not appear indicative of *in vivo* function.<sup>40</sup> Indeed, the specificity of Carabin (aka, Whacked ortholog TBC1D10C) has been controversial: it was first shown to act as a RasGAP,<sup>24</sup> while later studies indicate a Rab35-specific GAP activity<sup>23, 30, 32</sup>. Our *in vivo* genetic data for *whacked*, together with recent studies characterizing the function of all three human Whacked-like TBC proteins (TBC1D10A–C),<sup>23</sup> make a compelling case that this family of proteins acts as GAPs for Rab35. Further, our study establishes a role for classical vesicle trafficking proteins in seamless tube growth. Since seamless tubes but not multicellular or autacellular tracheal tubes are affected by mutations in *whacked* and Rab35, our study also establishes an *in vivo* cell type-specific requirement for trafficking genes in tube morphogenesis.

We conclude that Whacked and Rab35 regulate polarized growth of seamless tubes, and speculate that Whacked and Rab35 direct transport of apical membrane vesicles to the distal tip of terminal cell branches (when equilibrium is shifted toward active Rab35-GTP), or to a central location adjacent to the terminal cell nucleus (when equilibrium is shifted towards inactive Rab35-GDP). Analogous to its previously described roles in targeting vesicles to the immune synapse in T cells, the cytokinetic furrow in *Drosophila* S2 cells, and the neuromuscular junction in motor neurons, Rab35 would promote transport of vesicles from a recycling endosome compartment to the apical membrane. We further speculate that Breathless-FGFR activation at branch tips may couple terminal cell branching with seamless tube growth within that new branch (Figure S5f).

## METHODS

### Fly strains

EMS alleles of *whacked* were generated elsewhere<sup>17</sup> and are characterized below. *Minos* allele of *whacked* (<http://flybase.org>) is available from the Bloomington stock center (<http://flystocks.bio.indiana.edu>). Mosaic analyses: FRT82B, *wkd*<sup>220</sup>, FRTG13, *Lis1*<sup>G10.14</sup>, *Dhc64C*<sup>4-19</sup>, FRT2A; *Glued*<sup>1</sup>, FRT2A; and *dlic*<sup>1</sup> and *dlic*<sup>2</sup> FRT19A (kindly provided by Dr. Tadashi Uemura). Alleles of *singed* used *sn*<sup>36a</sup>, *sn*<sup>X2</sup>, and Df(1)c128. UAS-YFP::Rab (wild type, CA, and DN) strains were a gift from Jun Zhang and Matt Scott.<sup>22</sup> UAS-*whacked* RNAi strain was obtained from the VDRC (<http://stockcenter.vdrc.at/control/main>). UAS-



$\lambda$ Btl has been described,<sup>38</sup> and a second chromosome insertion was generated (ASG) by P-element mobilization. *crumbs::GFP* was a gift from Yang Hong.<sup>41</sup> UAS-*wkd* was generated by digesting *whacked* cDNA RE26521 (DGRC) with XhoI and BamHI and ligating to pUAST cut with XhoI and partially digested with BamHI. Orientation of the insert was confirmed by testing for the presence of the EcoRI site in the pUAST polylinker. Whacked::mKate2 fusion – the *whacked* cDNA was subcloned into pKS-bluescript, an NcoI site was introduced in place of the *whacked* stop codon. pmKate2 (Evrogen) was digested with NcoI and Not I, and inserted, in frame, downstream the *whacked* coding sequence. The *whacked::mKate2* fusion was cloned into pUAST. *whacked* genomic rescue construct: a 3909bp PCR product was amplified from a *w<sup>1118</sup>* genomic DNA (Qiagen DNeasy Kit) template using Phusion high fidelity DNA polymerase (New England Biolabs). The PCR product was cloned using a TopoTA cloning kit (Invitrogen). Clones were sequenced and mutant-free DNA was excised from the pCRII-Topo with Kpn I, and placed into pCasper4. UAS and genomic constructs were injected to generate transgenic strains according to standard protocols<sup>42</sup>, or by Genetic Services, Inc. pWG9.2, a second chromosome insertion of the *whacked* genomic DNA construct, rescued the tracheal defects and lethality associated with *wkd<sup>220</sup>/Df(3R)Exel6276* and *wkd<sup>MINOS</sup>/Df(3R)Exel6276* flies. Deficiency strains (<http://flybase.org>) are available from the Bloomington stock center, except for *Df(3R)pros235*, *Df(3R)pros640*, and *Df(3R)thoRI*, which were gifts from the Engels lab. *whacked* alleles. Although the U-turn phenotype is the predominant defect in *whacked* mutant animals, in our initial characterization of *whacked* we found that terminal cell seamless tubes often came to premature dead-ends (similar to the dynein motor mutants), and that the overall number of branches in each terminal cell was reduced (Supplemental Figure S2)<sup>17</sup>. Truncated tubes terminated in irregular shapes, leading us to name the gene *whacked*, to reflect the appearance that tubes had been crudely lopped off. However, extensive outcrossing of the *whacked<sup>220</sup>* strain resulted in a simplified phenotype in which a robust U-turn defect persisted but all other tube and branching defects were greatly reduced in frequency – this suggests that the principle phenotype of *whacked* mutants is exuberant seamless tube growth at branch tips, and also that loss of *whacked* sensitizes formation of seamless tubes to genetic background. Interestingly, these other phenotypes were also rescued by the *wkd* genomic rescue construct (see below).

### Positional cloning

Meiotic recombination placed *whacked* in the interval defined by the recessive markers *curled* (*cu*) and *stripe* (*sr*). Complementation tests against deficiency strains spanning the interval between *cu* and *sr* showed that *whacked* was uncovered by *Df(3R)MKX1* which deletes polytene bands 86C1 to 87B1-5. Recombinant chromosomes in which cross-overs occurred between *cu* and *sr* were typed with various RFLP SNP markers including 86E5 and 86F10 which defined a smaller (~300 kb) candidate interval for *whacked*. Strains with small defined chromosomal deletions spanning 86E to 86F10 were tested for complementation, establishing a ~75 kb segment of the chromosome in 86E14-17 as the location of the *whacked* gene.

### Primers

- (1) *whacked* genomic rescue construct

Forward genomic primer 5'-GGTACC CGTAAACTTGAACGTTGCCACC-3' and

Reverse genomic primer 5'-GGTACC GGTCTATGCACGTGAGCG-3',

(2,3) RFLP snp mapping – 86E5 (MspI: 2FRT parental chromosome is uncut, but the *ru h th st cu sr e ca* chromosome is cut).

pros1507F: 5'-CCACCAAACCTTCGGAATGCC-3'

pros2235B: 5'-TGGGGGTCGCTTATGCTTAGAC-3'

86F10 (NlaIV: 2FRT parental chromosome is cut, but the *ru h th st cu sr e ca* chromosome is uncut).

86F10F: 5'-ATTACGATGCCTTCGGTCCAC-3'

86F10B: 5'-AATGTCCTCACTTGTGCCACTG-3'

(4-9) *whacked* transcription unit sequence analysis:

TBC1F: 5'-TGCCACCTGGTTTTTGTCTAC-3'

TBC1B: 5'-CGAATGGGGGAAATCTCAATG-3'

TBC2F: 5'-TTTCACTGTCCCATTCGGTTG-3'

TBC2B: 5'-ATGTAGAGCCACTTCTTCTCCCGC-3'

TBC3F: 5'-CGAAATGGCTTCTATGGCGG-3'

TBC3B: 5'-TTCTTCAGCAGACCCTCCAGGATG-3'

TBC4F: 5'-GTCAGCGTGTGCGATGTGTAAG-3'

TBC4B: 5'-TGAACCAGTTTTGGGGTCACTC-3'

TBC5F: 5'-AAGGTGGCTCTGGTCATTATTGG-3'

TBC5B: 5'-AAACTTTTCAGGCTCGGGGG-3'

TBC6F: 5'-ATGATTACCACCCTGAGGCAGC-3'

TBC6B: 5'-TTTGGACGATGATGGCGACG-3'

**Sequence analyses**—*whacked* DNA and control DNA from the parental strain upon which *whacked* mutations were induced, were amplified by PCR and sequenced. In DNA from *whacked*<sup>PC24</sup> homozygous animals, a single nucleotide change from the parental chromosome was detected that corresponded to a T to A transversion, a missense mutation causing an amino acid substitution in the conserved TBC domain of Whacked. In DNA from *whacked*<sup>220</sup> animals, a C to T transition was detected, resulting in a nonsense mutation at the sixth codon position in the *whacked* coding sequence. Further support for the identity of *whacked* came from the subsequent identification of a third mutant allele, this one generated by the insertion of a Minos transposable element into the coding sequence of CG5344.<sup>43</sup> Terminal cells mutant for the Minos allele of *whacked* displayed a decreased number of branches and the U-turn phenotype.



## Immunohistochemistry

Antibodies used in these studies include: mouse  $\alpha$ -mRFP (1:1000, Abcam ab65856-100), rabbit  $\alpha$ -tRFP (anti-mKate2, 1:2000, Evrogen AB234), chick  $\alpha$ -GFP (1:1000, Invitrogen A10262), mouse  $\alpha$ -Ac-tubulin monoclonal antibody (1:2000, Sigma T6793), mouse  $\alpha$ - $\gamma$ -tubulin monoclonal antibody (1:1000, GTU-88, Sigma T6557). The Wkdpep rabbit polyclonal antibody was generated against the Wkd peptide, EHTRQKARRAKQKAQQE, but is used as a marker of terminal cell luminal membrane. Sera is not specific for Wkd as luminal membrane staining is still detected in *wkd* null (220/Df) and *wkd*<sup>MINOS</sup> larvae (the Minos insertion is within the last *wkd* exon, 5' of the nucleotides coding for the Wkd peptide antigen). DsRED, GFP and mKate2 were visualized by direct fluorescence in heat killed or fixed larvae, or by antibody staining of fixed and filleted larvae.

**Fascin and Egalitarian studies**—We carried out tests to determine whether *singed* might be the essential Rab35 effector in tracheal terminal cells for seamless tube morphogenesis. First, we asked whether terminal cells lacking Fascin displayed defects consistent with loss of Rab35 activity. We found that *singed* null terminal cells were entirely wild type in appearance (Figure S5b). Loss of *singed* also did not suppress the *whacked* mutant phenotype (Figure S5c,d). Likewise, loss of *singed* showed no apparent alteration of actin organization in terminal cells (Figure S5f,j). Furthermore, overexpression of Whacked (Figure S5h,i), or Rab35DN (data not shown), did not alter the terminal cell actin cytoskeleton, leading us to conclude that actin regulation is not a primary function of Wkd/Rab35 during seamless tube morphogenesis.

To test for a requirement for *egalitarian*, which serves as an adaptor for apically localized mRNA transport, we examined third instar larvae homozygous for *egl*<sup>1</sup>. Mutant terminal cells were indistinguishable from wild type (data not shown); however, we cannot rule out the possibility that maternal *egl* mRNA and protein masked a requirement for Egl function in seamless tube formation.

## Double mutant analyses

The following crosses were carried out: btl-Gal4, UAS-GFP; *wkd*<sup>220</sup>/TM3Sb, TubGal80 flies were crossed with UAS- $\lambda$ btl/CyO, UAS-DsRED; Df(3R)EXEL/TM6B, UAS-DsRED, or with UAS-Rab35DN/CyO, UAS-DsRED; Df(3R)EXEL/TM6B, UAS-DsRED. The progeny of these crosses that lacked DsRED expression were the experimental genotype, while sibling DsRED expressing larvae that lacked the Tubby phenotype served as *wkd* loss of function controls. The *sn* and *wkd* double mutant analysis was carried out as follows: Df(1)c128/FM7aGFP; Df(3R)EXEL6276/TM6B females were crossed to *singed*<sup>X2</sup>; *wkd*<sup>MI</sup>/TM6B males. The experimental genotypes were those progeny that lacked GFP and Tubby, while female siblings expressing GFP but lacking Tubby were used as *wkd* loss of function controls. In order to generate tracheal cells deficient for *dlic* and *wkd*, *dlic*<sup>1</sup>/FM7; *wkd*<sup>220</sup>/+ females were crossed to UAS-GFP RNAi, FRT19A FLP<sup>122</sup>; btl-Gal4, UAS-GFP; Df(3R)EXEL6276/+ males and progeny were heat shocked at 38.5°C for one hour after a four-hour egg collection. The *wkd*<sup>220</sup>/Df progeny were identified by their tracheal phenotype and were screened for *dlic* clones (GFP positive). To generate animals in which constitutive active Rab35 was expressed in *dlic* mutant terminal cells, *dlic*<sup>1</sup>/FM7; UAS-

Rab35CA females were crossed to TubGal80 FRT19A FLP<sup>122</sup>; btl-Gal4 UAS-GFP males and the progeny were heat shocked at 38.5°C for one hour after a four-hour egg collection. Positively marked clones were identified and scored for phenotype.

**Pulsed CD8::GFP experiment**—TubGal80ts flies were crossed with btl-Gal4, UAS-CD8-GFP flies, and the larvae were maintained at 18 °C until third larval instar. Larvae were then subjected to 1 hour heat shock at 38.5 °C to inactivate Gal80 and allow for btl-Gal4 driven expression of CD8-GFP. Larvae were filleted, fixed and stained (as described in methods) at 1 hour, 2 hours and 3 hours after temperature shift.

**Transgene Rescue of whacked viability**—The following crosses were carried out: (1) Rab35DN: UAS-Rab35DN; Df(3R)EXEL6276/TM6B X *breathless*-Gal4>DsRED/CyO; *wkd*<sup>220</sup>/TM6B. (2) Genomic Rescue: Two crosses were carried out – a) genomic rescue/S; Df(3R)EXEL6276 males were crossed to virgins that were *breathless*-Gal4>DsRED/CyO; *wkd*<sup>220</sup>/TM6B. (3) Whacked::mKate2: btl-Gal4, UAS-*wkd*::mKate2/CyO; Df(3R)EXEL6276/MKRS X Sp/CyO; *wkd*<sup>220</sup>/MKRS. Adults with the rescuing transgenes were scored.

**Live imaging of EB1::GFP**—Third-instar larvae of the genotype 4Xsrf-Gal4, UAS-EB1GFP were anesthetized with ether for fifteen minutes and imaged for up to 20 minutes on an Olympus Spinning Disk Confocal Microscope. Images were acquired with a 60X, 1.2 NA UPlanApo water immersion objective on a spinning disk confocal consisting of a Yokogawa CSU-X1 confocal scanner attached to an Olympus IX-81 microscope. The camera was an Andor iXon3 EMCCD camera and acquisition was controlled by MetaMorph 7.7. Images were collected at 2 frames/second for one minute. Direction of EB1 movement was determined by manual tracking of GFP fluorescence over a 10–20 second interval.

## Supplementary Material

Refer to Web version on PubMed Central for supplementary material.

## Acknowledgments

The authors would like to acknowledge: Danielle Willis, a former Stanford undergraduate student who helped with the rough mapping of *whacked*; Boaz Levi, who helped with the third chromosome screen; and Mark Krasnow, in whose lab the screen and early phases of these studies were carried out. We also thank Dr. Jun Zhang and the laboratories of Dr. Matt Scott and Dr. Hugo Bellen for making CA-Rab and DN-Rab stocks available to us prior to publication, the Engels lab for sharing Deficiency strains, and Mark Metzstein for sharing 4x-SRF-Gal4 flies. We thank Steve DiNardo, Chris Burd, Erfei Bi, and members of the Ghabrial and DiNardo labs for fruitful discussions. We thank Drs. Alondra Schweizer Burguete, Boaz Levi, and Nancy Speck for comments on the manuscript. JS-R was supported by NIH training grant 5-T32-HD007516-12 and subsequently, by an NIH postdoctoral fellowship (NRSA –GM090438-01). ASG gratefully acknowledges support from the University of Pennsylvania and the NIH (1R01GM089782-01A1). This work was supported in part by Basil O'Connor Starter Scholar Research Award Grant No. 5-FY09-43 from the March of Dimes Foundation.

## References

1. Samakovlis C, et al. Development of the Drosophila tracheal system occurs by a series of morphologically distinct but genetically coupled branching events. *Development*. 1996; 122:1395–1407. [PubMed: 8625828]

2. Ribeiro C, Neumann M, Affolter M. Genetic control of cell intercalation during tracheal morphogenesis in *Drosophila*. *Curr Biol*. 2004; 14:2197–2207. [PubMed: 15620646]
3. Buechner M. Tubes and the single *C. elegans* excretory cell. *Trends Cell Biol*. 2002; 12:479–484. [PubMed: 12441252]
4. Bar T, Guldner FH, Wolff JR. “Seamless” endothelial cells of blood capillaries. *Cell Tissue Res*. 1984; 235:99–106. [PubMed: 6697387]
5. Lubarsky B, Krasnow MA. Tube morphogenesis: making and shaping biological tubes. *Cell*. 2003; 112:19–28. [PubMed: 12526790]
6. Uv A, Cantera R, Samakovlis C. *Drosophila* tracheal morphogenesis: intricate cellular solutions to basic plumbing problems. *Trends Cell Biol*. 2003; 13:301–309. [PubMed: 12791296]
7. Gervais L, Casanova J. In vivo coupling of cell elongation and lumen formation in a single cell. *Curr Biol*. 2010; 20:359–366. [PubMed: 20137948]
8. Brodu V, Baffet AD, Le Droguen PM, Casanova J, Guichet A. A developmentally regulated two-step process generates a noncentrosomal microtubule network in *Drosophila* tracheal cells. *Dev Cell*. 2010; 18:790–801. [PubMed: 20493812]
9. Sutherland D, Samakovlis C, Krasnow MA. *branchless* encodes a *Drosophila* FGF homolog that controls tracheal cell migration and the pattern of branching. *Cell*. 1996; 87:1091–1101. [PubMed: 8978613]
10. Ribeiro C, Ebner A, Affolter M. In vivo imaging reveals different cellular functions for FGF and Dpp signaling in tracheal branching morphogenesis. *Dev Cell*. 2002; 2:677–683. [PubMed: 12015974]
11. Jarecki J, Johnson E, Krasnow MA. Oxygen regulation of airway branching in *Drosophila* is mediated by *branchless* FGF. *Cell*. 1999; 99:211–220. [PubMed: 10535739]
12. Berry KL, Bulow HE, Hall DH, Hobert O. A *C. elegans* CLIC-like protein required for intracellular tube formation and maintenance. *Science*. 2003; 302:2134–2137. [PubMed: 14684823]
13. Ulmasov B, Bruno J, Gordon N, Hartnett ME, Edwards JC. Chloride intracellular channel protein-4 functions in angiogenesis by supporting acidification of vacuoles along the intracellular tubulogenic pathway. *Am J Pathol*. 2009; 174:1084–1096. [PubMed: 19197003]
14. Grawe F, Wodarz A, Lee B, Knust E, Skaer H. The *Drosophila* genes *crumbs* and *stardust* are involved in the biogenesis of adherens junctions. *Development*. 1996; 122:951–959. [PubMed: 8631272]
15. Wodarz A, Hinz U, Engelbert M, Knust E. Expression of *crumbs* confers apical character on plasma membrane domains of ectodermal epithelia of *Drosophila*. *Cell*. 1995; 82:67–76. [PubMed: 7606787]
16. Waterman-Storer CM, et al. The interaction between cytoplasmic dynein and dynactin is required for fast axonal transport. *Proc Natl Acad Sci U S A*. 1997; 94:12180–12185. [PubMed: 9342383]
17. Ghabrial AS, Levi BP, Krasnow MA. A systematic screen for tube morphogenesis and branching genes in the *Drosophila* tracheal system. *PLoS Genet*. 2011; 7:e1002087. [PubMed: 21750678]
18. Levi BP, Ghabrial AS, Krasnow MA. *Drosophila* talin and integrin genes are required for maintenance of tracheal terminal branches and luminal organization. *Development*. 2006; 133:2383–2393. [PubMed: 16720877]
19. Albert S, Gallwitz D. Two new members of a family of Ypt/Rab GTPase activating proteins. Promiscuity of substrate recognition. *J Biol Chem*. 1999; 274:33186–33189. [PubMed: 10559187]
20. Albert S, Will E, Gallwitz D. Identification of the catalytic domains and their functionally critical arginine residues of two yeast GTPase-activating proteins specific for Ypt/Rab transport GTPases. *EMBO J*. 1999; 18:5216–5225. [PubMed: 10508155]
21. Strom M, Vollmer P, Tan TJ, Gallwitz D. A yeast GTPase-activating protein that interacts specifically with a member of the Ypt/Rab family. *Nature*. 1993; 361:736–739. [PubMed: 8441469]
22. Zhang J, et al. Thirty-one flavors of *Drosophila* rab proteins. *Genetics*. 2007; 176:1307–1322. [PubMed: 17409086]
23. Hsu C, et al. Regulation of exosome secretion by Rab35 and its GTPase-activating proteins TBC1D10A-C. *J Cell Biol*. 2010; 189:223–232. [PubMed: 20404108]

24. Pan F, et al. Feedback inhibition of calcineurin and Ras by a dual inhibitory protein Carabin. *Nature*. 2007; 445:433–436. [PubMed: 17230191]
25. Itoh T, Fukuda M. Identification of EPI64 as a GTPase-activating protein specific for Rab27A. *J Biol Chem*. 2006; 281:31823–31831. [PubMed: 16923811]
26. Ishibashi K, Kanno E, Itoh T, Fukuda M. Identification and characterization of a novel Tre-2/Bub2/Cdc16 (TBC) protein that possesses Rab3A-GAP activity. *Genes Cells*. 2009; 14:41–52. [PubMed: 19077034]
27. Chevallier J, et al. Rab35 regulates neurite outgrowth and cell shape. *FEBS Lett*. 2009
28. Chua CE, Lim YS, Tang BL. Rab35--a vesicular traffic-regulating small GTPase with actin modulating roles. *FEBS Lett*. 2010; 584:1–6. [PubMed: 19931531]
29. Echard A. Membrane traffic and polarization of lipid domains during cytokinesis. *Biochem Soc Trans*. 2008; 36:395–399. [PubMed: 18481967]
30. Gao Y, et al. Recycling of the Ca<sup>2+</sup>-activated K<sup>+</sup> channel, KCa2.3, is dependent upon RME-1, Rab35/EPI64C, and an N-terminal domain. *J Biol Chem*. 2010; 285:17938–17953. [PubMed: 20360009]
31. Kouranti I, Sachse M, Arouche N, Goud B, Echard A. Rab35 regulates an endocytic recycling pathway essential for the terminal steps of cytokinesis. *Curr Biol*. 2006; 16:1719–1725. [PubMed: 16950109]
32. Patino-Lopez G, et al. Rab35 and its GAP EPI64C in T cells regulate receptor recycling and immunological synapse formation. *J Biol Chem*. 2008; 283:18323–18330. [PubMed: 18450757]
33. Sato M, et al. Regulation of endocytic recycling by *C. elegans* Rab35 and its regulator RME-4, a coated-pit protein. *EMBO J*. 2008; 27:1183–1196. [PubMed: 18354496]
34. Shim J, et al. Rab35 mediates transport of Cdc42 and Rac1 to the plasma membrane during phagocytosis. *Mol Cell Biol*. 2010; 30:1421–1433. [PubMed: 20065041]
35. Uytterhoeven V, Kuenen S, Kasproicz J, Miskiewicz K, Verstreken P. Loss of skywalker reveals synaptic endosomes as sorting stations for synaptic vesicle proteins. *Cell*. 2011; 145:117–132. [PubMed: 21458671]
36. Zhang J, Fonovic M, Suyama K, Bogyo M, Scott MP. Rab35 controls actin bundling by recruiting fascin as an effector protein. *Science*. 2009; 325:1250–1254. [PubMed: 19729655]
37. Lee S, Kolodziej PA. The plakin Short Stop and the RhoA GTPase are required for E-cadherin-dependent apical surface remodeling during tracheal tube fusion. *Development*. 2002; 129:1509–1520. [PubMed: 11880359]
38. Lee T, Hacohen N, Krasnow M, Montell DJ. Regulated Breathless receptor tyrosine kinase activity required to pattern cell migration and branching in the *Drosophila* tracheal system. *Genes Dev*. 1996; 10:2912–2921. [PubMed: 8918892]
39. Pfeffer S. Filling the Rab GAP. *Nat Cell Biol*. 2005; 7:856–857. [PubMed: 16136184]
40. Fuchs E, et al. Specific Rab GTPase-activating proteins define the Shiga toxin and epidermal growth factor uptake pathways. *J Cell Biol*. 2007; 177:1133–1143. [PubMed: 17562788]
41. Huang J, Zhou W, Dong W, Watson AM, Hong Y. Directed, efficient, and versatile modifications of the *Drosophila* genome by genomic engineering. *Proc Natl Acad Sci U S A*. 2009; 106:8284–8289. [PubMed: 19429710]
42. Rubin GM, Spradling AC. Genetic transformation of *Drosophila* with transposable element vectors. *Science*. 1982; 218:348–353. [PubMed: 6289436]
43. Bellen HJ, et al. The BDGP gene disruption project: single transposon insertions associated with 40% of *Drosophila* genes. *Genetics*. 2004; 167:761–781. [PubMed: 15238527]

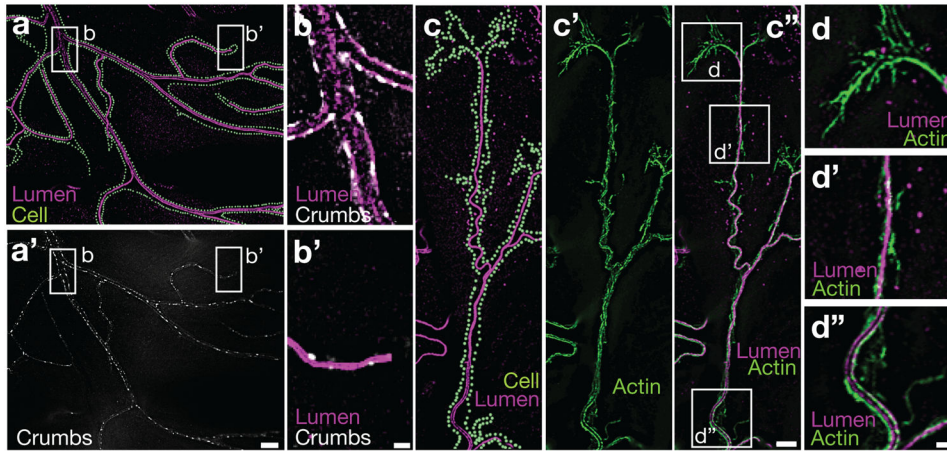


**FIGURE 1. The lumenal membrane of tracheal terminal cells has apical identity**

(a) A portion of a wild type terminal cell is shown, with the cell shape outlined by dots (Cell, light green) – cell outline layer was made by tracing actin::RFP staining with the gain increased sufficiently to visualize basolateral actin. The terminal cell is stained with  $\alpha$ -Wkdpep sera, revealing the lumenal membrane (Lumen, magenta) of seamless tubes. (a') Staining (Crumbs, white) against a functional Crumbs::GFP fusion protein knocked into the endogenous *crumbs* locus demonstrates that the lumenal membrane of terminal cell seamless tubes is apical. White boxes in (a, a') labeled b and b' marquee the terminal cell soma and a branch tip, respectively, and are shown enlarged in (b, b'). Merged images of Crumbs (white) and lumenal membrane (Lumen, magenta) co-staining are shown. Subcellular localization of actin relative to the seamless tube is examined in (c – c''). In (c), a portion of a terminal cell (Cell, light green dots) containing a branched seamless tube (Lumen, magenta) is shown. In (c'), the subcellular distribution of actin (Actin, green) is shown. In (c''), a merged image is shown. The white boxes labeled (d, d', and d'') highlight distinct domains of actin localization that are shown enlarged in (d-d''): (d) filopodial actin, (d') basolateral actin, and (d'') apical actin. Scale bars for a, a' in a'; for c, c', c'' in c'' = 10  $\mu$ m and in b, b' and d'' for b, b' and for d, d', d'', respectively = 2  $\mu$ m.



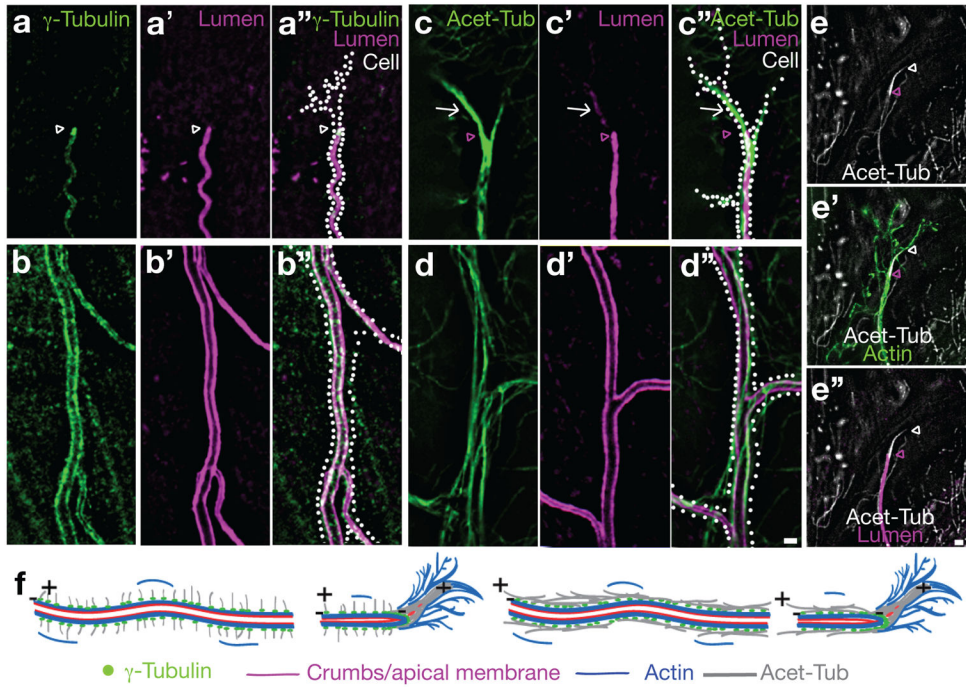


### FIGURE 2. The terminal cell microtubule cytoskeleton is polarized

Terminal cell outlines (determined as in Figure 1) are indicated (Cell, white dots). (a, b) The subcellular distribution of  $\gamma$ -tubulin is shown in a typical wild type terminal cell.  $\gamma$ -tubulin ( $\gamma$ -Tub, green) lines the seamless tube and is enriched at the blind-end of the tube found at the tip of the terminal cell (a). Costaining of  $\gamma$ -tubulin and apical membrane (magenta, a', b') is shown (a'', b''). (c, d) The subcellular distribution of acetylated microtubules (Acet-Tub, green) is shown. Acetylated microtubule bundles run parallel the apical membrane (magenta, c', d'). Costaining is shown (c'', d''). We note that apical membrane fragments (white arrow) discontinuous with the seamless tube are found to line acetylated microtubule tracts extending beyond the seamless tube blind end (magenta arrowhead). (e) The relationship between acetylated microtubules (white), apical membrane (Lumen, magenta) and actin rich filopodia (Actin, green) at branch tips is shown. Acetylated microtubules extend beyond (white arrowhead) the blind-end (magenta arrowhead) of the seamless tube. Actin-based filopodial projections extend beyond both the seamless tube and the stable microtubule tract. These data (and those from Figure 1) are summarized in the schematic diagrams shown in (f). In the panel on the left, microtubules are shown oriented perpendicular to the axis of the tube while in the panel on the right, microtubules are shown oriented parallel to the long axis of the tube. Either or both microtubule arrangements may be present. Scale bars for a-d are in d'' and for e, e' and e'' are in e'' and = 2  $\mu$ m.



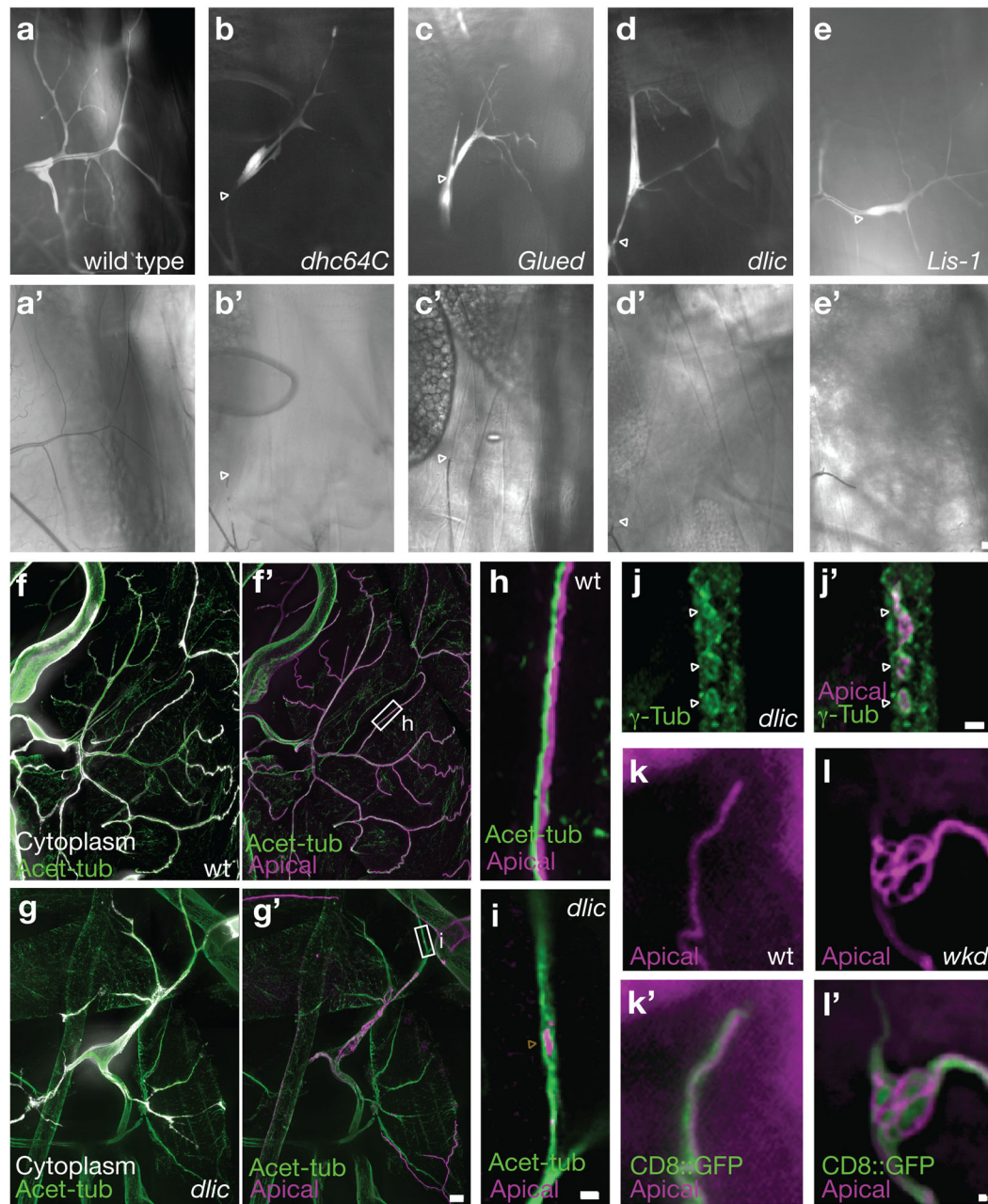


**FIGURE 3. Seamless tube growth is blocked or is overly exuberant in dynein motor complex and whacked mutants, respectively**

(a–d) Positively marked (GFP, white) mutant terminal cells were identified in mosaic animals. Cells mutant for dynein motor complex components made branched cellular extensions, but had little or no air-filled seamless tubes (arrowheads indicate the position beyond which gas-filling of tubes is not detected, a'–e'). To determine if acetylated microtubules (green) were present within terminal cells lacking air-filled tubes, wild type control (f, f') and *dlic* (g, g') mosaic animals were filleted, fixed and stained. Homozygous terminal cell clones (f, g) were marked with GFP (white). Apical membrane (Apical –  $\alpha$ -Wkdpep – magenta) staining reveals seamless tube remnants near the terminal cell nucleus

(g') of mutant terminal cells, but not near branch tips (compare f',g'). In (h,i), high magnification images of seamless tubes from wild type and *dlic* mutant terminal cells (f', g'; marquee area), respectively. In wild type (h), continuous seamless tube was present along the acetylated microtubule bundle. In *dlic* mutant cells, apical membrane was absent except for small bits of discontinuous tube that could be detected adjacent to acetylated microtubules (i, arrowhead). We found that such discontinuous bits of tube were able to organize  $\gamma$ -tubulin around them, but that  $\gamma$ -tubulin localization was mostly lost in dynein complex mutant terminal cells, with staining present diffusely throughout the cell (j, j' compare to Figure 2a,b). As compared to wild type animals (k, k'), seamless tubes in *whacked* terminal cells showed excessive growth at branch tips (i, i'), resulting in a "U-turn" phenotype, in which seamless tube extended through the cytoplasm in a series of 180 degree turns. Scale bars for a-e' in e'; for f-g' in g' = 10  $\mu\text{m}$ ; for h and i in i, for j,j' in j' and for k-l' in l' = 2  $\mu\text{m}$ .

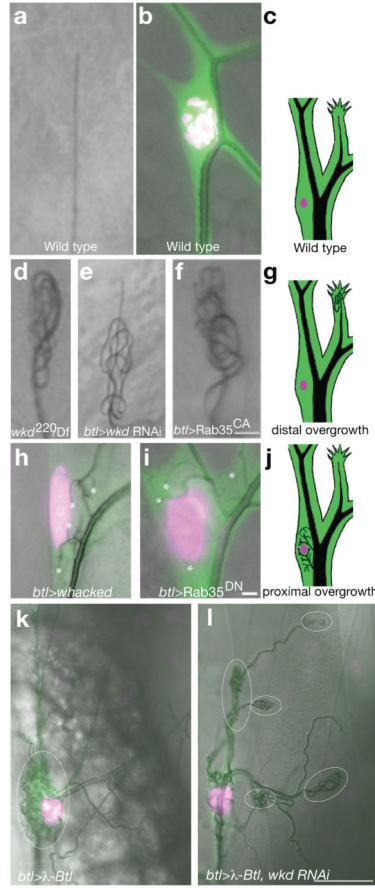


#### FIGURE 4. Whacked and Rab35 polarize seamless tube growth

In (a, d-f), brightfield micrographs revealing gas-filled terminal cell seamless tubes are shown. In (b, h,i, k and l), fluorescent micrographs labeling the terminal cell cytoplasm (green) and nucleus (magenta) are superimposed on a brightfield image. In (a) and (b) wild type terminal cell branch tip (a) and soma (b) are shown. In (c), a schematic illustrates the position and distribution of seamless tubes in wild type terminal cells. In *wkd* (d), *wkd* RNAi (e), or Rab35CA (f) terminal cell tips, growth of seamless tubes appears to outpace growth of cellular extensions, resulting in a tangle of gas-filled tubes coiled in the tip cytoplasm. In (g), the distal seamless tube overgrowth seen in (d – f) is illustrated in a schematic diagram. In terminal cells over-expressing *wkd* (h), or Rab35DN (i), ectopic gas-filled seamless tubes (\*) are observed surrounding the terminal cell nucleus. This proximal overgrowth phenotype is illustrated in the schematic in (j). In (k), a terminal cell expressing an activated FGFR ( $\lambda$ -*breathless*) produces ectopic gas-filled seamless tubes (outlined with dashed white oval) surrounding the terminal cell nucleus (magenta), much like (although more extreme than) overexpression of *wkd* or Rab35DN. In (l), a sibling larva expressing a *whacked* RNAi transgene in addition to  $\lambda$ -Btl shows abundant ectopic tubes (white ovals) at branch tip positions rather than around the nucleus (magenta). Scale bars in f (for a, d–f), i (for b, h, and i) = 5 microns, and l (for l, k) = 50 microns.

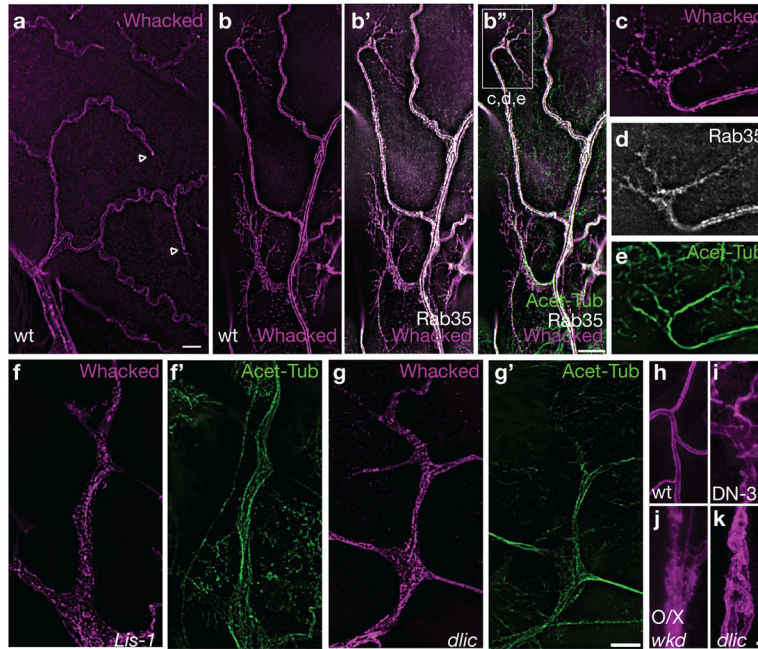


**FIGURE 5. Subcellular distribution of Wkd and Rab35, and the role of minus-end transport in seamless tube growth**

In wild type terminal cells (a–e) Whacked::mKate2 fusion protein (Whacked, magenta), is enriched apically, especially at branch tips (arrowheads). In comparison (b',b'',d), YFP::Rab35 (white) is more broadly distributed, but also apically enriched. Whacked and Rab35 show extensive co-localization (b'), and also overlay with acetylated microtubule tracts (Acet-Tub, green). At branch tips (marqueed area in b''), Wkd (c) and Rab35 (d) are adjacent to acetylated microtubules (e), but also decorate actin-based filopodial processes (see Figure S3). In dynein motor complex mutants (*Lis-1*, f,f'; *dlic* g,g'), Whacked is dispersed throughout the cytoplasm and often detected on basolateral membrane. Although not excluded from areas with acetylated microtubule bundles, Whacked is not enriched along them (f'', g''). In (h–k),  $\alpha$ -Wkdpep is used to stain the apical membrane of seamless tubes; in the soma surrounding the terminal cell nucleus of wild type cells (h), single seamless tubes are found growing into each cytoplasmic extension, whereas terminal cells expressing a dominant negative Rab35 isoform (i), overexpressing (O/X) wild type Whacked (j), or mutant for dynein motor complex components such as *dlic* (k) have ectopic seamless tubes. Scale bars in a for a, in g' for b–g' = 10  $\mu$ m ; in e for c–e = 1  $\mu$ m; and in k for h–k = 2  $\mu$ m.